ARTICLE IN PRESS

Pressure effect on the structural, electronic, optical and elastic properties of $Zn_{0.75}Be_{0.25}O$ from first-principles calculations

Q1 F. Elhamra [a], S. Lakel [a,b,*], H. Meradji [c]

[a] Laboratory of Physical Materials – University of LAGHOUAT, BP 37G Laghouat, Algeria
[b] Laboratoire de Matériaux Semi Conducteurs et Métalliques «LMSM», Université de Biskra, Algeria
[c] Laboratoire de Physique des Rayonnements, Université Badji Mokhtar Annaba, Algeria

A B S T R A C T

In this work we focused on the effect of the pressure on the material because of its great importance in different environments. A first principles study has been performed to calculate the structural, electronic, optical and elastic properties of $Zn_{0.75}Be_{0.25}O$ under different pressures. Our results of the transitions from wurtzite (B4) to rocksalt (B1) structure occur around 11.04 GPa and 13 GPa for ZnO and $Zn_{0.75}Be_{0.25}O$, respectively. The lattice constants decrease and the band gap increases with increasing pressure. The valence band maximum moves to lower energy, whereas the conduction band minimum moves to higher energy with increasing pressure, so the band gap broadens. The curve shape for optical parameters is almost unchanged within creasing pressure, but all the peaks moves to higher energy (blueshift). Our results provide a theoretical reference for the design of UV devices comprising Be-doped ZnO. Finally, our results are predictions at different pressures.

© 2015 Published by Elsevier GmbH.

1. Introduction

In recent years, scientists have focused on semiconductors since it has many advantages on the industrial and technological level. For example, we took in our study ZnO because it is a semiconductor and has many properties such as the wide band gap and large excitation binding energy. In addition, ZnO can be used in ultraviolet optoelectronic applications, solar cell [1]. Besides, we can make alloy by mixing ZnO with materials (BeO, CdO and MgO...). ZnO-based can be used in quantum wells, piezoelectric semiconductors, and super lattices.

We have studied $Zn_{1-x}Be_xO$ to increase the band gap, which can occurs through replacing a Zn atom by a Be atom, in addition, we know that BeO has the same hexagonal symmetry with ZnO. There are many investigations in recent years on $Zn_{1-x}Y_xO$ (Y = Mg, Be) as follows, Xu et al. [2] have studied the electronic structures of wurtzite ZnO, BeO, MgO and p-type doping in $Zn_{1-x}Y_xO$, the investigated each of the elasticity, band structure, and piezoelectricity of $Be_xZn_{1-x}O$ alloys are presented by Duan et al. [3]. There are also previous studies focused on Be-composition effect on structural, electronic and optical properties of $Be_xZn_{1-x}O$ alloys by Bing et al. [4], while, Maouche et al. [5] have been focused on the dependence of structural properties of ZnO on high pressure, however, Cui et al. [6] also have been investigated the structural and electronic properties of ZnO under high pressure. We found that the first-principles calculations of optical properties of BeO in its ambient and high-pressure phases were studied by Groh et al. [7]. In addition, from the first-principles calculations of phase transition and elastic properties of BeO under pressure are presented by Yu et al. [8].

Although there is a large number of theoretical calculations on BeZnO, most of the properties calculated at 0 GPa. In recent years, most studies have focused on the effect of pressure on the material, because the materials have applications in different environments with different pressures. In these papers, we study the structural, electronic, optical and elastic properties under high pressure.

The present work is organized as follow: a description of the calculation scheme is given in Section 2, the results are discussed in Section 3. Finally, we give a summary of this work in Section 4.

2. Computational methods

In this study, all the calculations were conducted through the use of the CASTEP code [9,10], based on the density functional theory (DFT) [11]. For the exchange correlation function, we used the generalized gradient approximation (GGA) in the scheme of Perdew–Burke–Ernzerh of (PBE) [12]. Pseudo atomic calculations are performed for each of Be: $2s^2$, Zn: $3d^{10}4s^2$ and O: $2s^22p^4$. We took the Ultrasoft pseudopotentials [13] to model ion–electron

* Corresponding author. Tel.: +213 0771409403.
E-mail address: said.lakel@yahoo.fr (S. Lakel).
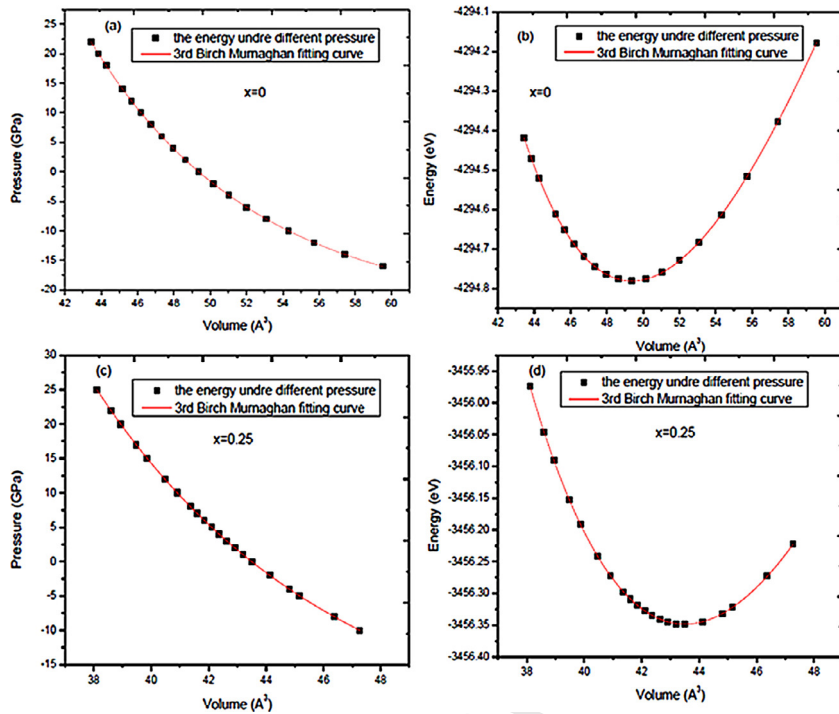
Fig. 1. Birch–Murnaghan equation of state for ZnO and $Zn_{0.75}Be_{0.25}O$, including E–V and P–V.

interactions. In this work, we have used two basic parameters as the kinetic cutoff energy for plane waves 730 eV and $5 \times 5 \times 6$ k-point mesh according to the Monkhorst–Pack [14] for supercell system. The geometry optimization was calculated by using Brodydene Fletchere Goldfarbe Shanno (BFGS) minimization technique [15]. The total energy was converged to less than 5×10^{-7} eV/atom and the maximum ionic Hellmanne Feynman force of per atom was converged to less than 0.01 eV/Å. In addition, for more accurate results for each of the electronic and optical properties, we have worked to increase the k-points to $8 \times 8 \times 10$.

In order to study the structural, electronic, optical and elastic properties of $Zn_{0.75}Be_{0.25}O$ under pressure. First, we used $2 \times 2 \times 1$ supercell ZnO, where two Zn atoms were replaced by the two of Be atoms in the supercell.

3. Results and discussion

3.1. Structural properties

The variation of total energy as a function of volume has been calculated for the optimized structure using the generalized gradient approximation (GGA), as shown in Fig. 1b–d. From Fig. 1b–d, we note that the energy decreases with increasing volume to reach the lowest value (the minimum energy E_0) at the optimal volume V_0. And also of the curve, we note that the energy increases with increasing volume after the optimal volume and deduce from it system is unstable. Whereas, the minimum energy E_0 agrees optimal volume V_0.

The energy–volume (E–V) curve in Fig. 1b–d can be obtained by fitting the calculated E–V results to the Birch–Murnaghan EOS [16], **Q2** which is given in Eq. (1):

$$E(V) = E_0 - \frac{9}{16}B_0 \left[(4 - B') \frac{V_0^3}{V^2} - (14 - 3B') \frac{V_0^{7/3}}{V^{4/3}} + (16 - 3B') \frac{V_0^{5/3}}{V^{2/3}} \right] \quad (1)$$

The pressure–volume (E–V) curve in Fig. 1a–c is fitted to the Birch–Murnaghan equation of state (EOS), as shown in Eq. (2):

$$P(V) = \frac{3}{2}B_0 \left[\left(\frac{V_0}{V}\right)^{7/3} - \left(\frac{V_0}{V}\right)^{5/3} \right]$$

$$\times \left\{ 1 + \frac{3}{4}(B' - 4) \left[\left(\frac{V_0}{V}\right)^{2/3} - 1 \right] B' \right\} \quad (2)$$

The bulk modulus B_0 and its pressure derivative B' are determined by fitting the calculated E–V and P–V data to the Birch–Murnaghan equation of state (EOS). Our results of the lattice parameters, the bulk modulus B_0 (GPa) and its first derivative B' with other calculations for ZnO and $Zn_{0.75}Be_{0.25}O$ at $P = 0$ GPa and $T = 0$ K are presented in Table 1. Through Fig. 1a and b, we note that our results are in good agreement with results obtained by Feng et al. [17] for ZnO.

Our results of the lattice parameters (a, c) for ZnO are in good agreement with the experimental value [18] ($a = 3.25$ Å, $c = 5.21$ Å) and the theoretical results [17,19,20]. In addition, we can see that our results are in excellent agreement with previous theoretical values [4,23] for $Zn_{0.75}Be_{0.25}O$. Obviously, due to the non-existence of the experimental and theoretical results of its pressure derivative B' for comparison, our results are considered as a new reference for further investigation.

We have calculated the variations of the enthalpy as a function of pressure for ZnO and $Zn_{0.75}Be_{0.25}O$ of two phases (WZ and RS), which are presented in Fig. 2. In addition, we know that the enthalpy plays an important role for studding the stability of phase. When the enthalpies of the B4 and B1 phases are equal that we can calculated the transition pressure as follows $(H_{B4}(P_t) = H_{B1}(P_t))$. It can be seen that our results of the transitions from B4 to B1 occur around 11.04 GPa and 13 GPa for ZnO and $Zn_{0.75}Be_{0.25}O$, respectively. Our results of the phase transition pressure from B4 to B1 are shown in Table 2 for ZnO and $Zn_{0.75}Be_{0.25}O$ along with previous experimental and theoretical data, which shows the calculated results are in well agreement with latest experimental

Table 1

Q3 The lattice constants a and c (Å), the bulk modulus B_0 (GPa) and its first derivative B' of $Zn_{0.75}Be_{0.25}O$ compared to other theoretical values.

Structure	a (Å)		c (Å)			B (GPa)		B' (GPa)	
	This work	Other calcul.	This work	Other calcul.		This work	Other calcul.	This work	Other calcul.
ZnO	3.281	3.295[a] 3.289[b] 3.282[e]	5.296	5.317[a] 5.308[b] 5.293[e]	E–V EOS fitted P–V EOS fitted	129.30 129.35	145.41[e] 131.5[c] 145.48[e]	4.42 4.44	4.47[e] 4.4[c] 4.51[e]
$Zn_{0.75}Be_{0.25}O$	3.135	3.134[f]	5.109	5.076[f]	E–V EOS fitted P–V EOS fitted	143.28 143.26		4.20 4.19	

[a] Ref. [19].
[b] Ref. [20].
[c] Ref. [21].
[d] Ref. [22].
[e] Ref. [17].
[f] Ref. [23].
[g] Ref. [4].
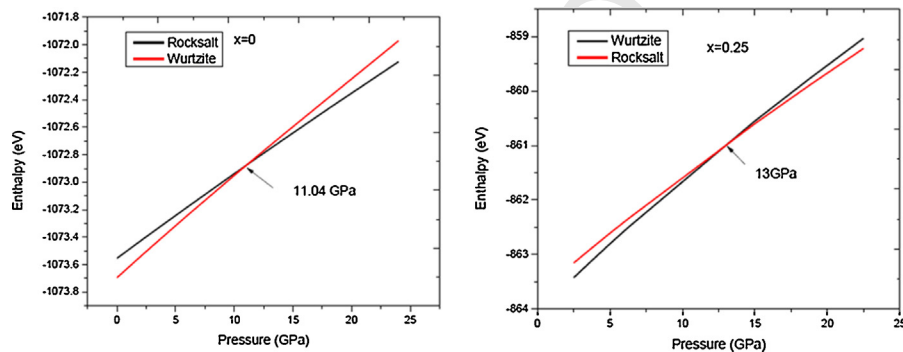
Fig. 2. Enthalpy as a function of pressure for ZnO and $Zn_{0.75}Be_{0.25}O$ of two phases (WZ and RS).

Table 2

Transition pressure (P_t) of ZnO and $Zn_{0.75}Be_{0.25}O$ from the B4 to the B1 phase.

Structures	P_t (GPa)		
	Present work	Experimental	Other calculations
ZnO	11.04	10[a], 8.7[b]	11.439[c], 11.59[d], 9.013[c], 11.8[e]
$Zn_{0.75}Be_{0.25}O$	13		

[a] Ref. [24].
[b] Ref. [25].
[c] Ref. [20].
[d] Ref. [26].
[e] Ref. [27].

value and previous theoretical calculations for ZnO. Due to the nonexistence of the experimental and theoretical results of the phase transition pressure from B4 to B1 for comparison of $Zn_{0.75}Be_{0.25}O$, our results are considered as a new reference for further investigation.

We choose the pressure less than the transition pressure for each of ZnO and $Zn_{0.75}Be_{0.25}O$ to avoid possible phase transitions. The variations in lattice constants with the pressure between 0 and 8 GPa using GGA and are presented in Fig. 3. We noted that the lattice constants decrease with the increase of pressure. We know that the difficulty of pressure on the crystal structure refer to increase the strength of repulsion between atoms and conclude that each of the lattice parameters and volume decreased with increasing pressure. Where we found the relationship between them from the quadratic function as follow:

$$\begin{cases} a_{Zn_{0.75}Be_{0.25}O} = 0.0001\,P^2 - 0.0078\,P + 3.1 \\ c_{Zn_{0.75}Be_{0.25}O} = 0.00013\,P^2 - 0.01\,P + 5.1 \end{cases}$$

3.2. Band structure

The calculated energy band structures of $Zn_{0.75}Be_{0.25}O$ along with the high-symmetry points of the Brillouin zone at 0 GPa and 8 GPa by GGA function are shown in Fig. 4a and b. Through Fig. 4, we note that each of the valence band maximum (VBM) and the conduction band minimum (CBM) are located at G point, resulting in a direct band gap (G–G). From Fig. 5a it is clear that the result of the band gap for ZnO (0.747 eV) is in well agreement with the other calculations (0.75 eV [28] and 0.735 eV [29]), but much smaller than the experimental data [30] 3.44 eV. While, our result of the band gap of $Zn_{0.75}Be_{0.25}O$ (1.589 eV) agrees with the theoretical value (1.645 eV) [23] at P = 0 GPa. It is easy to observe that the band gap increases with the increase of the pressure, as shown in Fig. 3b. When the pressure increases, the conduction band moves to the higher-energy region. However, the valence band tends to shift toward the low-energy region, so the band gap broadens. In addition, the energy band gap of $Zn_{0.75}Be_{0.25}O$ can be expressed as a function of pressure by the following formula:

$$E_g^{Zn_{0.75}Be_{0.25}O}(P) = -0.00021\,P^2 + 0.016\,P + 1.6$$

4

F. Elhamra et al. / Optik xxx (2015) xxx–xxx
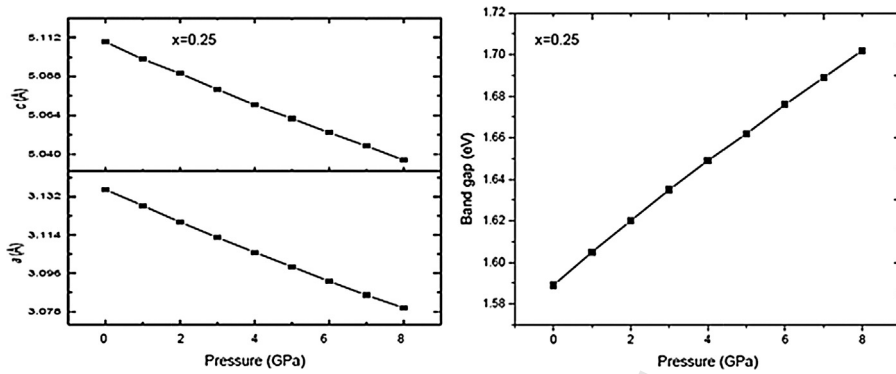
Fig. 3. Lattice constants a and c (a) and band gap (b) as a function of pressure.
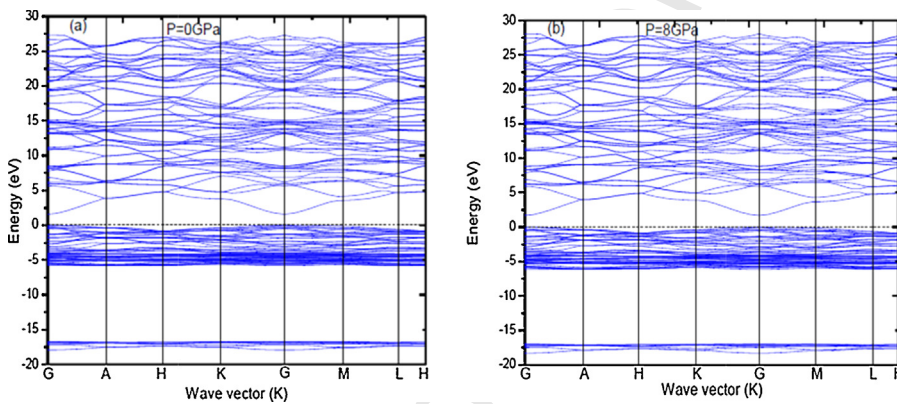
Fig. 4. Band structures of $Zn_{0.75}Be_{0.25}O$ at (a) $P = 0$ GPa and (b) $P = 8$ GPa.

The partial density of states (PDOS) has a role in determining the information about the electronic nature of the material. We note that the partial density of states gives the contribution of each atom as follows Zn (3d/4s), Be (2s) and O (2s/2p). It is seen from Fig. 5b that the largest contribution lies in the orbital O: 2p at the upper valence band (−3.40 to 0 eV). Whereas, the biggest contribution represents in the orbital of Zn: 3d at the lower valence band (−6.55 to −3.40 eV). While, it seems the strongest contribution appears in the orbital of O: 2s at region between −18.22 eV and −16.55 eV for ZnO. However, the partial density of states of $Zn_{0.75}Be_{0.25}O$ at 0 and 8 GPa are presented in Fig. 6. From Fig. 6, we can see that at zero pressure, the valence band region from −18.26 eV to 0 eV consists of three regions. The first region from −18.26 eV to −16.71 eV, we observe that the largest contribution lies in the orbital O: 2s with the smallest contributions of orbitals (Zn: 4s/3d and Be: 2s). Whereas,

the second region between −6.37 eV and −3.27 eV, we can see that the biggest contribution represents in the orbital of Zn: 3d with the least contributions of the orbitals (Zn: 4s, Be: 2s and O: 2p), while the third region from −3.27 to 0 eV, the strongest contribution represents in the orbital O: 2p with negligible contributions of orbitals (Zn: 3d and Be: 2s). When the pressure increases, the orbitals of the conduct band (CB) have moving toward higher energy. While, the orbitals of the valence band (VB) moving to lower energy, which results in an increase of the band gap.

3.3. Optical properties

We know that the relationship $\varepsilon(\omega) = \varepsilon_1(\omega) + i\varepsilon_2(\omega)$ has a role in describing the optical properties of materials. Whereas, the imaginary part $\varepsilon_2(\omega)$ of the dielectric function can be obtained from the
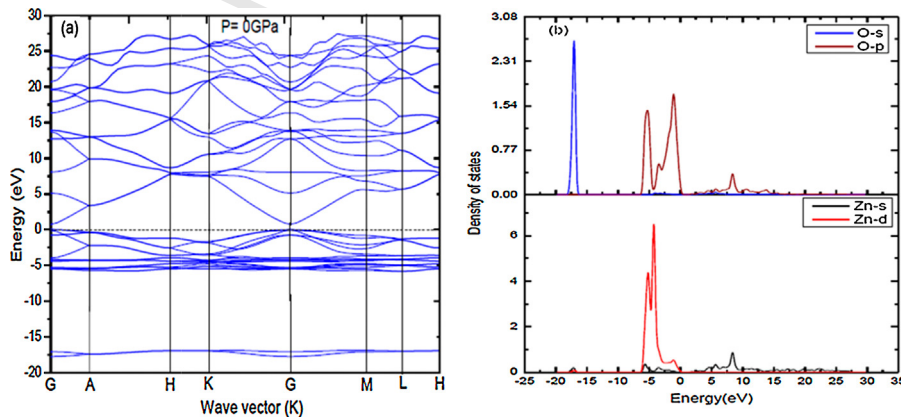
Fig. 5. Band structure (a) and partial (PDOS) density of states (b) of ZnO at $P = 0$ GPa.
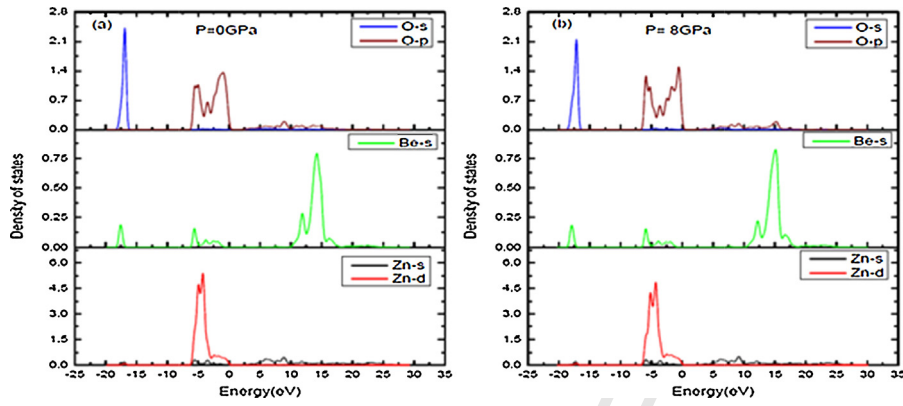
Fig. 6. Partial (PDOS) density of states for $Zn_{0.75}Be_{0.25}O$ at (a) $P = 0$ GPa and (b) $P = 8$ GPa.
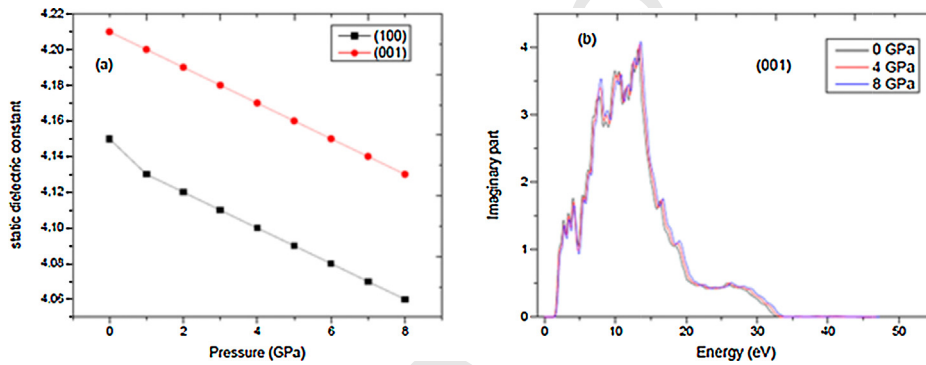
Fig. 7. The static dielectric constant along polarization directions $(0\,0\,1)$ and $(1\,0\,0)$ (a) and the imaginary part of the dielectric function along polarization direction $(0\,0\,1)$ (b) of $Zn_{0.75}Be_{0.25}O$ as a function of pressure.

momentum matrix elements between the occupied and unoccupied electronic states. Also, the real part $\varepsilon_1(\omega)$ can be calculated by using the Kramers–Kronig relation. In addition to the rest of the optical parameters such as the absorption coefficient $\alpha(\omega)$, refractive index $n(\omega)$ and extinction coefficient $k(\omega)$ can be calculated from Imaginary part and real part of dielectric function, Where is given according to the following equations [31]:

$$k(\omega) = \frac{\left[\sqrt{\varepsilon_1(\omega)^2 + \varepsilon_2(\omega)^2} - \varepsilon_1(\omega) \right]^{1/2}}{\sqrt{2}} \qquad (3)$$

$$n(\omega) = \frac{\left[\sqrt{\varepsilon_1(\omega)^2 + \varepsilon_2(\omega)^2} + \varepsilon_1(\omega) \right]^{1/2}}{\sqrt{2}} \qquad (4)$$

$$\alpha(\omega) = \frac{2\sqrt{2}\pi \left[\sqrt{\varepsilon_1(\omega)^2 + \varepsilon_2(\omega)^2} - \varepsilon_1(\omega) \right]^{1/2}}{\lambda} \qquad (5)$$

In this section, we have been calculated each of the static dielectric constant, the imaginary part of the dielectric function, the static refraction index, extinction coefficient and absorption coefficient as a function of pressure of $Zn_{0.75}Be_{0.25}O$, as shown in Figs. 7–9 respectively.

Our results of the static dielectric constant $\varepsilon_1(0)$ and the static refraction index $n(0)$ are listed in Table 3 along with the theoretical value [4] at $P = 0$ GPa for ZnO and $Zn_{0.75}Be_{0.25}O$. It can be observed that our results are in agreement with the theoretical data at $P = 0$ GPa. Unfortunately, there are no experimental results. Through our results, we observed that the largest value for the static dielectric constant lies in along polarization direction $(0\,0\,1)$ compared to the direction $(1\,0\,0)$. We can see that the static dielectric constant decreases with the increase of the pressure in

Table 3
Dielectric constant $(\varepsilon_1(0))$ and index of refraction $(n(0))$ of ZnO and $Zn_{0.75}Be_{0.25}O$ at $P = 0$ GPa.

	$\varepsilon_1(0)$ $(1\,0\,0)$	$(0\,0\,1)$	$n(0)$ $(0\,0\,1)$
ZnO	6.83	5.54	2.35
	9.47[a]	5.49[a]	2.35[a]
$Zn_{0.75}Be_{0.25}O$	4.147	4.214	2.05
	4.78[a]	3.98[a]	1.98[a]

[a] Ref. [4].

both along polarization directions $(0\,0\,1)$ and $(1\,0\,0)$. From Fig. 7, we note that the imaginary part of the dielectric function starts at about 1.340, 1.412 and 1.50 eV along polarization direction $(0\,0\,1)$ for $Zn_{0.75}Be_{0.25}O$ at 0, 4 and 8 GPa, respectively, which is in good agreement with the theoretical result at $P = 0$ GPa [4]. Unfortunately, there are no experimental results and theoretical data for comparison at high-pressure, our results are considered as a new reference for further investigation.

Fig. 8a and b shows each of the static refraction index $n(0)$ and the extinction coefficient $k(\omega)$ at different pressures. Through Table 3, it can be noted that our results are in well agreement with the theoretical data at $P = 0$ GPa for ZnO and $Zn_{0.75}Be_{0.25}O$ in along polarization direction $(0\,0\,1)$. In addition, we can be observed that static refraction $n(0)$ decreases with the pressure increasing. From Fig. 8b, We found that the first critical points of extinction coefficient are located at 1.389, 1.439 and 1.539 eV along polarization direction $(0\,0\,1)$ for $Zn_{0.75}Be_{0.25}O$ at 0, 4 and 8 GPa, respectively, which agrees with the theoretical result at $P = 0$ GPa [4].

We have calculated the absorption coefficient along polarization directions $(0\,0\,1)$ and $(1\,0\,0)$ at different pressures as shown in Fig. 9a and b. For along polarization direction $(0\,0\,1)$, it can
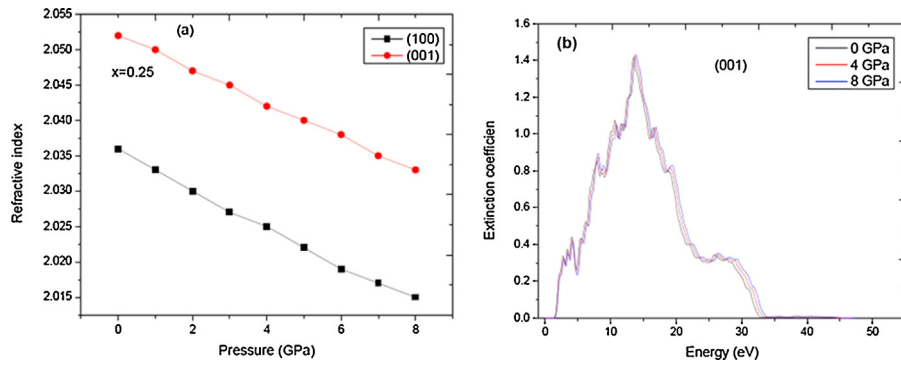
Fig. 8. The static refraction index along polarization directions (0 0 1) and (1 0 0) (a) and the extinction coefficient along polarization directions (0 0 1) (b) of $Zn_{0.75}Be_{0.25}O$ as a function of pressure.
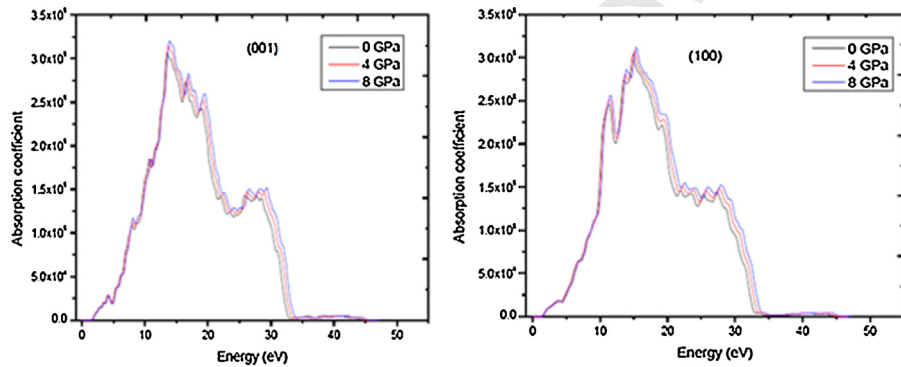
Fig. 9. Absorption curves along polarization direction (0 0 1) (a) and absorption curves along polarization direction (1 0 0) (b) of $Zn_{0.75}Be_{0.25}O$ as a function of pressure.

be observed that the absorption starts at about 1.563, 1.638 and 1.712 eV. Whereas, the first critical points of absorption start at about 1.364, 1.414 and 1.539 eV along polarization direction (1 0 0) at 0, 4 and 8 GPa, respectively. The starting of the peak for absorption coefficient is in good agreement with the theoretical result at $P = 0$ GPa [4]. From Fig. 9a and b, we note that the absorption band broadens with the pressure increasing.

3.4. Elastic properties

Elastic constants characterize the ability of a material to deform under any small stresses. The effect of strain on the physical properties is also important in terms of getting some knowledge of the mechanical properties of the materials. It also helps us in the calculation each of the specific heat, melting point, Debye temperature, thermal expansion coefficient and mechanical properties.

The change of elastic constants with pressure between 0 and 8 GPa is shown in Fig. 10. From Fig. 10, we can see that the elastic constants C_{11}, C_{12}, C_{13} and C_{33} increase rapidly with the increase of pressure, while, the elastic constant C_{44} decreases slowly with the pressure increasing. In addition, we know that the elastic properties have a role in determining the mechanical stability of any solid structure by stability criteria. Whereas, stability criteria of the hexagonal structure is given in the following equation Eq. (1) [32,33].

$$C_{11} > 0, \quad C_{11} - C_{12} > 0, \quad C_{44} > 0, \quad (C_{11} + C_{12})C_{33} - 2C_{13}^2 > 0$$

$$(6)$$

Our results agree well with the Eq. (1). And from it we can deduce that the $Zn_{0.75}Be_{0.25}O$ crystal is mechanically stable at different pressures. In addition, the elastic constants and mechanical properties of ZnO and $Zn_{0.75}Be_{0.25}O$ at 0 GPa are given in Table 4,
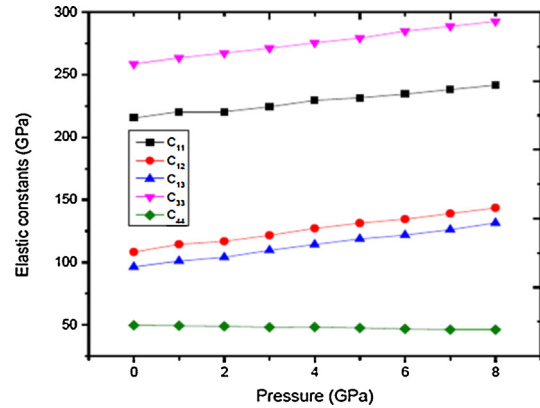
Fig. 10. Calculated elastic constants of $Zn_{0.75}Be_{0.25}O$ as a function of pressure.

together with the available theoretical data and experimental value.

In addition, each of the shear modulus G and bulk modulus B can be calculated by using the following approximations Voigt, Reuss and Voigt–Reuss–Hill [34–37], as show in the Eqs. (2)–(7).

$$G_V = \frac{1}{5}(2C_{11} + C_{33} - C_{12} - 2C_{13}) + \frac{1}{5}(2C_{44} + C_{66}) \qquad (7)$$

$$B_V = \frac{2}{9}(C_{11} + C_{12} + 2C_{13} + C_{33}/2) \qquad (8)$$

$$B_R = \frac{1}{2(S_{11} + S_{33}) + 2(S_{12} + 2S_{13})} \qquad (9)$$

$$G_R = \frac{15}{4(2S_{11} + S_{33}) - 4(S_{12} + 2S_{13}) + 3(2S_{44} + S_{66})} \qquad (10)$$

$$B_H = (1/2)(B_V + B_R) \qquad (11)$$

Table 4
Calculated elastic constants C_{ij} and mechanical properties for ZnO and $Zn_{0.75}Be_{0.25}O$ at zero pressure, including the reported theoretical value from reference.

	C_{11}	C_{12}	C_{13}	C_{33}	C_{44}	B	E	G	ν
ZnO	188.96	110.32	90.41	200.97	36.87	129.00	113.83	41.25	0.355
	206[a]	120[b]	118[a]	211[a]	44.3[a]	131.5[c]	111.2[d]	44[e]	0.349[f]
	184[g]	93[g]	77[g]	206[g]	56[g]				
	215.7[h]	136.1[h]	122.7[h]	249.6[h]	38.6[h]				
$Zn_{0.75}Be_{0.25}O$	215.41	108.27	96.35	258.62	49.67	143.25	148.09	55.77	0.328
	231[h]	136.5[h]	120[h]	306[h]	50[h]	167.48[h]	227.63[h]		

[a] Ref. [38].
[b] Ref. [39].
[c] Ref. [17].
[d] Ref. [40].
[e] Ref. [41].
[f] Ref. [42].
[g] Ref. [43].
[h] Ref. [3].
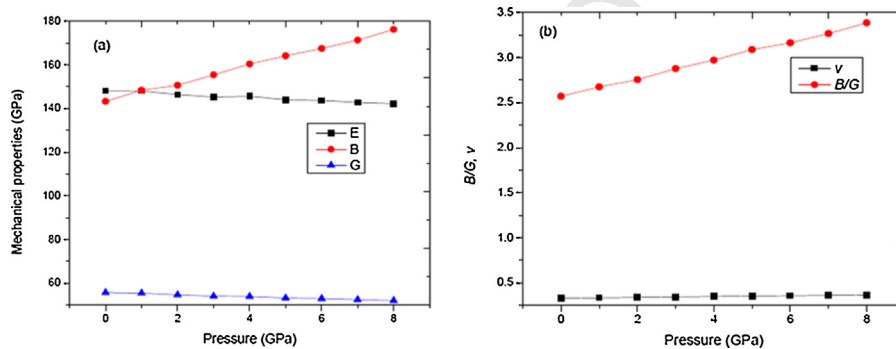
Fig. 11. Calculated mechanical properties (a), the B/G (b) and Poisson's ratio ν (c) of $Zn_{0.75}Be_{0.25}O$ as a function of pressure.

$$G_H = (1/2)(G_V + G_R) \tag{12}$$

The Young's modulus and Poisson's ratio are calculated from shear and bulk modulus by using approximation of Voigt–Reuss–Hill [34].

$$E = \frac{9BG}{3B + G} \tag{13}$$

$$\sigma = \frac{3B - 2G}{2(3B + G)} \tag{14}$$

The variation of mechanical properties and the ratio of bulk modulus to shear modulus for $Zn_{0.75}Be_{0.25}O$ with increasing pressure are shown in Fig. 11. From Fig. 11, we found that the bulk modulus (B) and Poisson's ratio (ν) increase as the increase of the pressure. However, the shear modulus (G) and Young's modulus (E) decrease slowly with the pressure increasing. We know that the ratio of bulk modulus to shear modulus (B/G) is important for understanding ductility and brittleness of the material. Moreover, the ratio of shear modulus to bulk modulus (B/G) has been evaluated by Pugh [44]. Whereas, the critical value of (B/G) is about 1.75. If $B/G < 1.75$, the material behaves in a brittle manner, otherwise, the material behaves in a ductile. Through Fig. 11, we note that the value of the (B/G) is larger than the critical value, indicating a ductile nature of $Zn_{0.75}Be_{0.25}O$. Additionally, Poisson's ratio plays an important role for the description of the bonding forces [45]. For central force solids the value of Poisson's ratio (ν) is between 0.25 and 0.5 [46]. It can be noted that the value of Poisson's ratio is between 0.25 and 0.5, which indicates that inter atomic forces are central forces in $Zn_{0.75}Be_{0.25}O$. Through Table 4, our results are in well agreement with the theoretical values and experimental data [17,38–44] at $P = 0$ GPa.

4. Conclusions

In this work, first-principles DFT calculations revealed that lattice constants (a, c) of $Zn_{0.75}Be_{0.25}O$ decrease with increasing pressure. The valence band maximum moves to lower energy, whereas the conduction band minimum moves to higher energy with increasing pressure, so the band gap broadens. As we conclude that the band gap increases with the pressure increasing. The curve shape for the optical parameters are almost unchanged as the pressure is increased, but all the peaks move to higher energy. We have also calculated the values of static dielectric constants $\varepsilon_1(0)$ and static refraction index $n(0)$ along polarization directions $(0\,0\,1)$ and $(1\,0\,0)$. We observed that the values of $\varepsilon_1(0)$ and $n(0)$ decrease with an increase in pressure. We calculated the values of elastic constants and mechanical properties at different pressures. Through the results we observed that the elastic constants C_{11}, C_{12}, C_{13} and C_{33} increase rapidly with the increase of pressure, while, the elastic constant C_{44} decreases with the pressure increasing. We conclude that our results at 0 GPa are in good agreement with theoretical values and experimental data. Finally, Our results provide a theoretical reference for Be-doped ZnO applications such as band gap modulation for UV devices.

References

[1] K. Keis, E. Magnusson, H. Lindstrom, S.E. Lindquist, A. Hagfeldt, Sol. Energy Mater. Sol. Cells 73 (2002) 51.
[2] Q. Xu, X.-W. Zhang, W.-J. Fan, S.-S. Li, J.-B. Xia, Comput. Mater. Sci. 44 (2008) 72–78.
[3] Y. Duan, H. Shi, L. Qin, Phys. Lett. A 372 (2008) 2930–2933.
[4] L. Bing, X. Zhou, R.-F. Linghu, X.-L. Wang, X.-D. Yang, Chin. Phys. B 20 (3) (2011) 036104.
[5] D. Maouche, F. Saad Saoud, L. Louail, Mater. Chem. Phys. 106 (2007) 11–15.
[6] S. Cui, W. Feng, H. Hu, Z. Feng, Y. Wang, J. Alloys Compd. 476 (2009) 306–310.
[7] D. Groh, R. Pandey, M.B. Sahariah, E. Amzallag, I. Baraille, M. Rérat, J. Phys. Chem. Solids 70 (2009) 789–795.

[8] B.-R. Yu, J.-W. Yang, H.-Z. Guo, G.-F. Ji, X.-R. Chen, Physica B 404 (2009) 1940–1946.

[9] M.D. Segall, P.J.D. Lindan, M.J. Probert, C.J. Pickard, P.J. Hasnip, S.J. Clark, M.C. Payne, J. Phys. Condens. Matter 14 (2002) 2717.

[10] P.L. Mao, B. Yu, Z. Liu, F. Wang, Y. Ju, J. Magn. Alloy 1 (2013) 256.

[11] W. Kohn, L. Sham, Phys. Rev. A 140 (1965) 1133.

[12] J.P. Perdew, K. Burke, W. Ernzerhof, Phys. Rev. Lett. 77 (1996) 3865.

[13] D. Vanderbilt, Phys. Rev. B 41 (1990) 7892.

[14] H.J. Monkhorst, J.D. Pack, Phys. Rev. B 13 (1976) 5188.

[15] B.G. Pfrommer, M. Côté, S.G. Louie, M.L. Cohen, J. Comp. Physiol. 131 (1997) 133–140.

[16] F. Birch, J. Geophys. Res. 83 (1978) 1257.

[17] F. Wang, J. Wu, C. Xia, C. Hu, C. Hu, P. Zhou, L. Shi, Y. Ji, Z. Zheng, X. Liu, J. Alloys Compd. 597 (2014) 50–57.

[18] O. Madelung, M. Schultz, H. Weiss, Numerical Data and Functional and Relationships in Science and Technology, Springer-Verlag, Berlin, 1982, pp. 97.

[19] X. Su, P. Si, Q. Hou, X. Kong, W. Cheng, Physica B 404 (2009) 1794–1798.

[20] F.-G. Kuang, X.-Y. Kuang, S.-Y. Kang, M.-M. Zhong, A.-J. Mao, Mater. Sci. Semicond. Process. 23 (2014) 63–71.

[21] A. Schleife, F. Fuchs, J. Furthmüller, F. Bechstedt, Phys. Rev. B73 (2006) 2452–2512.

[22] J.E. Jaffe, J.A. Snyder, Z. Lin, A.C. Hess, Phys. Rev. B 62 (2000) 1660–1665.

[23] Z. Yongping, C. Zhigao, L. Yu, W. Qingyun, W. Zhenzhen, H. Zhigao, J. Semicond. 0253-4177 (2008) 12-2316-06.

[24] L. Gerward, J. Staun Olsen, J. Synchrotron Radiat. 2 (1995) 233.

[25] H. Karzel, W. Potzel, M. Köfferlein, W. Schiessl, M. Steiner, U. Hiller, G.M. Kalvius, D.W. Mitchell, T.P. Das, P. Blaha, K. Schwarz, M.P. Pasternak, Phys. Rev. B 53 (1996) 11425–11438.

[26] M.P. Molepo, D.P. Joubert, Phys. Rev. B 84 (2011) 094110.

[27] B. Meyer, D. Mark, Phys. Rev. B 67 (2003) 035403.

[28] K. Osuch, E.B. Lombardi, W. Gebicki, Phys. Rev. B 73 (2006) 075202.

[29] Z. Ming, H.Z. Chuan, S. Jiang, Chin. Phys. B 20 (2011) 017101.

[30] A. Mang, K. Reimann, S. Rubenacke, Solid State Commun. 94 (1995) 251.

[31] F.W. Xie, P. Yang, P. Li, L.Q. Zhang, Opt. Commun. 285 (2012) 2660–2664.

[32] M. Born, K. Huang, Dynamical Theory of Crystal Lattices, Oxford University Press, London, 1954.

[33] M.S. Islam, A.K.M.A. Islam, Physica B 406 (2011) 275.

[34] H.C. Chen, L.J. Yang, Physica B 406 (2011) 4489.

[35] Z.M. Sun, S. Li, R. Ahuja, J.M. Schneider, Solid State Commun. 129 (2004) 589.

[36] Z.J. Lin, Y.C. Zhou, M.S. Li, J. Mater. Sci. Technol. 23 (2007) 721.

[37] R. Hill, Proc. Phys. Soc. 65 (1952) 350.

[38] O. Madelung (Ed.), Semiconductors: Data Handbook, third ed., Springer, Berlin, 2004.

[39] O. Madelung (Ed.), Landolt-Börnstein, New Series, Group III: Solid State Physics Low Frequency Properties of Dielectric Crystals: Elastic Constants, vol. 29a, Springer, Berlin, 1993.

[40] S.O. Kucheyev, J.E. Bradby, J.S. Williams, C. Jagadish, M.V. Swain, Appl. Phys. Lett. 80 (2002) 956.

[41] Z. Liu, X. He, Z. Mei, H. Liang, L. Gu, X. Duan, X. Du, J. Phys. D: Appl. Phys. 47 (2014) 105303 (8 pp.).

[42] Y. Gao, Z.L. Wang, Nano Lett. 9 (2009) 1103–1110.

[43] R. Chowdhury, S. Adhikari, F. Scarpa, Physica E 42 (2010) 2036–2040.

[44] S.F. Pugh, Philos. Mag. 45 (1954) 823–843.

[45] B. Mayer, H. Anton, E. Bott, et al., Intermetallics 11 (2003) 23.

[46] H.Z. Fu, D.H. Li, F. Peng, T. Gao, X.L. Cheng, Comput. Mater. Sci. (2008) 774.